

ELASTIC WAVE MODELLING IN ANISOTROPIC MEDIA USING THE
SPECTRAL-ELEMENT METHOD

by

Catherine Ellen Sinclair

B.Eng (Computer Systems)

Department of Physics
School of Chemistry and Physics
The University of Adelaide
SA 5005, Australia

Submitted in partial fulfillment of the requirements
for the degree of Doctor of Philosophy

June 2009

Table of Contents

List of Tables	vi
List of Figures	vii
Abstract	xii
Statement	xiv
Acknowledgements	xvi
Chapter 1 Introduction	1
1.1 Modelling Seismic Waves	1
1.2 Thesis Objectives	11
1.3 Thesis Outline	11
Chapter 2 Frequency-Domain and Time-Domain Numerical Seismic Modelling	13
2.1 Introduction	13
2.2 Frequency-Domain Modelling	14
2.2.1 The 3-D Equation for a General Anisotropic Medium	14
2.2.2 The 2.5-D Equation for a General Anisotropic Medium	16
2.2.3 The 2.5-D Equation for a Vertical Transversely Isotropic Medium	17
2.2.4 The 2.5-D Equation for a Tilted Transversely Isotropic Medium	19
2.2.5 The 3-D Equation for an Orthorhombic Medium	23
2.3 Time-Domain Modelling	24
2.3.1 The 2.5-D Time-Domain Equation for a VTI Medium	24
2.3.2 Time Marching	25
2.3.3 Source Signal	26
2.4 The Frequency-Domain 3-D Spectral-Element Equations	27
2.5 The Frequency-Domain 2.5-D Spectral-Element Equations for TI media	31
2.6 The Time-Domain 2.5-D Spectral-Element Equations	33
Chapter 3 Absorbing or Transmitting Boundary Conditions and Layers	35
3.1 Introduction	35
3.2 Viscous Boundary Conditions	36
3.3 Simple Frequency-Domain Perfectly Matched Layers	44
3.3.1 PMLs for Transversely Isotropic Media	45
3.4 Perfectly Matched Layers using the Decomposed Gradient Operator	50
3.4.1 Derivation of the Second-order PML Equations	52

3.4.2	The Complete PML Wave Equation	54
3.4.3	Field Splitting in the Time-Domain	55
3.4.4	The Frequency-Domain PML Wave Equation	56
3.4.5	Decomposed Displacement Gradient Tensors and Stresses	57
3.4.6	Decomposed Equations of Motion	59
Chapter 4	Spectral-Element Method for Element Integration	63
4.1	Introduction	63
4.2	2.5-D Spectral-Element Formulation	63
4.2.1	Outline of the Approach	63
4.2.2	Defining Elements with Shape Functions	64
4.2.3	Finding the Jacobian	67
4.2.4	Higher Order Interpolation Functions and their Derivatives	70
4.2.5	Transformation of Element Equations to Local Coordinates	71
4.2.6	Gauss-Lobatto Quadrature	74
4.2.7	Discretising the Subintegrals	75
4.2.8	The Set of 2.5-D Subintegral Types and their 2-D Patterns	79
4.3	3-D Spectral-Element Formulation	79
4.3.1	A Brief Outline of the 3-D Approach	79
4.3.2	Higher Order Interpolation Functions and their Derivatives	83
4.3.3	Transformation of Element Equations to Local Coordinates	84
4.3.4	Discretising the Subintegrals	87
4.3.5	The Set of 3-D Subintegral Types and their 3-D Patterns	91
4.4	The Gauss-Lobatto Formulation of Viscous Boundaries	93
Chapter 5	Computational Implementation	97
5.1	Introduction	97
5.2	Classification of Subintegrals	97
5.3	A High Level View of the 2.5-D Algorithm	99
5.4	Assembly of the System Matrix	100
5.4.1	System Matrix Structure	100
5.4.2	A Binary Tree System Matrix	102
5.5	3-D Modelling	103
5.6	Implementation of PML Subintegrals	105
5.6.1	2-D implementation	105
5.6.2	3-D PMLs	106
5.6.3	2.5-D Time-Domain PMLs	107
5.7	Matrix Solvers	111
5.7.1	Using Solvers on Linux	111
5.7.2	Converting a Complex Matrix to a Purely Real Matrix	112
5.7.3	Distributed Memory vs. Shared Memory	113
5.7.4	Direct versus Iterative Solvers	115
Chapter 6	Verification of Numerical Modelling Results using Analytic Solutions	122
6.1	Introduction	122
6.2	Homogeneous Isotropic Full Space	122
6.3	Homogeneous VTI Full Space	124

6.4	Transformation to the Frequency-Wavenumber Domain via FFT	125
6.5	Critical Wavenumbers in the Transformed Analytic Solution	130
6.6	Comparison of Numerical Results with the Analytic Solutions	135
Chapter 7	Numerical Modelling Results and Discussion	144
7.1	Introduction	144
7.2	Frequency Domain Results for Homogeneous Media	145
7.2.1	2-D Isotropic Media	146
7.2.2	2-D VTI Media	151
7.2.3	2.5-D Isotropic Media	153
7.2.4	2.5-D VTI Media	159
7.2.5	Tilted TI Media	160
7.2.6	2-D Anisotropic Crystals	171
7.2.7	3-D Frequency-Domain Modelling Results	171
7.2.8	Modelling with a Free Surface	173
7.3	Frequency Domain Results for Simple Heterogeneous Media	180
7.3.1	Isotropic media	180
7.3.2	VTI media	181
7.4	Time-Domain Modelling Results	189
7.4.1	Homogeneous Isotropic Media	189
7.4.2	Homogeneous VTI media	189
7.4.3	Heterogeneous VTI media	197
7.4.4	3-D Time-Domain Modelling Results	199
7.5	Evaluation of the Absorbing Boundary Techniques	201
7.5.1	Time-Domain Absorbing Boundaries	201
7.5.2	Frequency-Domain Absorbing Boundaries in Isotropic Media	205
7.5.3	Performance of Perfectly Matched Layers in Nulls	206
7.5.4	Stability of Perfectly Matched Layers	210
7.6	Memory Requirements of Frequency-Domain and Time-Domain Modelling	213
Chapter 8	Critical Wavenumbers and Wavenumber Sampling in 2.5-D Modelling	216
8.1	Introduction	216
8.2	Evanescent Energy	219
8.3	Wavenumber Sampling	219
8.4	Critical Wavenumber Values	225
8.5	Phase and Group Velocities in Anisotropic Media	227
8.6	The Nature of Critical Wavenumbers in Anisotropic Media	230
8.7	Critical Wavenumbers in Simple Inhomogeneous Media	233
8.7.1	Suppressing the Effect of Critical Wavenumbers	235
8.7.2	The Effect of Reflections at the Interface	245
8.8	The Effect of Critical Wavenumbers on the Frequency-Domain Solution	254
8.9	Removal of Singularities via the Introduction of a Slight Attenuation	255
8.10	Are There Poles in Practice at the Critical Wavenumbers?	256
8.11	Towards a Wavenumber Sampling Strategy	257
8.12	Are There Critical Wavenumbers in the Time-Domain?	259

Chapter 9	Conclusions and Outlook	268
9.1	Major Outcomes	268
9.2	Future Research	270
Appendix A	The High Accuracy of the Spectral-Element Method	273
Appendix B	Integration by Parts for 2.5-D Spectral-Element Modelling	277
Appendix C	Explanation of Boundary Integral Notation	279
Appendix D	Displacement Gradient Tensor vs. Symmetric Strain Tensor	282
Appendix E	Simple Frequency-Domain Perfectly Matched Layers in 3-D	284
Appendix F	Plots of the Analytic Solutions	287
F.1	Plots of the Isotropic Analytic Solution	287
F.2	Plots of the VTI Analytic Solution	287
Appendix G	Further Details of the Computational Implementation	296
G.1	The Element Data Structure	296
G.2	Coding a Binary Tree System Matrix	298
G.3	A User Makefile	301
Appendix H	Removing the Singularity in 2.5-D Elastic Wave Modelling by Introducing Slight Attenuation	303
H.1	Introduction	303
H.2	Critical Wavenumbers and Singularities	304
H.3	Removing the Singularity	306
H.4	Preliminary Results for the Acoustic Case	307
H.5	Conclusions	308
Glossary		314
References		315

List of Tables

3.1	Classification of stresses	41
3.2	Boundary Vectors	42
3.3	Normal and Parallel Stresses - left and right	59
3.4	Normal and Parallel Stresses - top and bottom	59
4.1	Gauss Lobatto patterns for a rectangular element	80
4.2	Gauss-Lobatto patterns for a cuboid element	92
4.3	The set of 2.5-D viscous boundary expressions	96
5.1	Variation of the damping function	106
7.1	The elastic coefficients and velocities for a selection of isotropic media.	145
7.2	The elastic coefficients and Thomsen parameters of four VTI media.	145
7.3	Identification of some of the wave modes in Figure 7.56	198
8.1	Properties of isotropic media A and D at 300 Hz	226
8.2	Velocities and wavenumbers in a VTI medium	233
8.3	Max and Min phase and group velocities VTI medium	233
8.4	Max and Min phase and group velocities VTI medium	233
8.5	Max and Min phase and group velocities VTI medium	233
8.6	Properties of four isotropic media at 300 Hz	236
8.7	Properties of two VTI media at 300 Hz	245
9.1	272

List of Figures

1.1	Forward modelling and inversion	2
1.2	Illustration of a single 2-D spectral element	7
1.3	Stresses acting on the elementary cube	9
1.4	Equilibrium condition for stresses	10
2.1	Rotation of right-handed coordinate system	20
2.2	A Ricker wavelet	27
2.3	A set of 5th order 1-D Lagrange polynomials	28
3.1	Normal and tangential stresses on boundary points within elements	37
3.2	Boundary Vectors on artificial boundary - 3-D	39
3.3	Boundary Vectors on artificial boundary - 2.5-D	40
3.4	Classification of boundary stresses	41
3.5	Classification of Absorbing Layers	44
3.6	Normals to the absorbing layer	51
3.7	A PML damping function	51
4.1	Relationship between local and global coordinates in 2-D	66
4.2	Relationship between local and global coordinates in 3-D	82
5.1	A 2X2 element system	101
5.2	System matrix for a 2X2 element system	101
5.3	Part of a binary tree row	103
5.4	Element layers of a 3-D model, showing the C-style element numbering.	104
5.5	Layout for the nodes in a cuboid element	105
5.6	Classification of absorbing boundary layers in a 2-D element.	105
5.7	Classification of absorbing boundary layers for a 3-D model.	106
5.8	Inner Node layout in system matrix for time-domain PMLs	110
5.9	Boundary node layout in system matrix for time-domain PMLs	110
5.10	A Distributed Memory System	113
5.11	A Shared Memory System	113
5.12	Memory usage ILUPACK	118
5.13	Memory usage estimates SCSL	119
5.14	Memory usage PARDISO	120
5.15	Execution time ILUPACK	121
6.1	Spatial Fourier transform of the analytic solution	125
6.2	The circular symmetry of an even input sequence for FFT	126

6.3	The symmetry of the spatially Fourier transformed isotropic analytic solution	127
6.4	The symmetry of the spatially Fourier transformed isotropic analytic solution	128
6.5	The symmetry of the spatially Fourier transformed isotropic analytic solution	129
6.6	Spatially FFT'd y component of isotropic analytic solution	131
6.7	Zooming in on critical wavenumbers, y component, isotropic analytic solution	132
6.8	Spatially FFT'd z component of isotropic analytic solution	132
6.9	Zooming in on critical wavenumbers, z component, isotropic analytic solution	133
6.10	Spatially Fourier transformed x component of isotropic analytic solution . .	133
6.11	Zooming in on the S critical wavenumber, x component, analytic solution .	134
6.12	Isotropic frequency-wavenumber-domain solution vs. FFT'd analytic	136
6.13	Isotropic frequency-wavenumber-domain solution vs. FFT'd analytic	137
6.14	Isotropic frequency-wavenumber-domain solution vs. FFT'd analytic	138
6.15	Comparison 3-D modelling with analytic - homogeneous, isotropic	139
6.16	Comparison 3-D modelling with analytic - homogeneous, isotropic	139
6.17	Comparison 3-D modelling with analytic - homogeneous, isotropic	140
6.18	VTI Frequency-wavenumber-domain solution vs. FFT'd analytic	141
6.19	VTI Frequency-wavenumber-domain solution vs. FFT'd analytic	142
6.20	VTI Frequency-wavenumber-domain solution vs. FFT'd analytic	143
7.1	2-D solution for homogeneous isotropic medium A, x-directed source	147
7.2	2-D solution for homogeneous isotropic medium A, y-directed source	148
7.3	2-D solution for homogeneous isotropic medium A z-directed source	149
7.4	Comparison of rotated wavefields	150
7.5	2-D solution for homogeneous VTI medium, y-directed source	152
7.6	Solution at $k_y = 1.0$ for homogeneous isotropic medium A, x-directed source	154
7.7	Solution at $k_y = 1.0$ for homogeneous isotropic medium A, y-directed source	154
7.8	Solution at $k_y = 1.0$ for homogeneous isotropic medium A, z-directed source	155
7.9	Comparison of rotated wavefields wavenumber 1.0	156
7.10	Comparison of rotated wavefields wavenumber 1.0	157
7.11	Solution at wavenumber $k_y = 1.5$ for homogeneous isotropic medium A . .	158
7.12	Isotropic wavefronts - medium A	158
7.13	VTI solution for a real y-directed source at $k_y = 0.25$	161
7.14	VTI wavefronts - medium E	162
7.15	Phase and group velocities in VTI medium E	162
7.16	VTI solution for a real y-directed source at $k_y = 0.25$	163
7.17	VTI wavefronts - medium F	164
7.18	Phase and group velocities in VTI medium F	164
7.19	VTI medium H. Solution for a real x-directed source at $k_y = 0.1$	165
7.20	VTI medium H. Solution for a real y-directed source at $k_y = 0.1$	166
7.21	VTI medium H. Solution for a real z-directed source at $k_y = 0.1$	167
7.22	VTI wavefronts - medium H	168
7.23	Phase and group velocities in VTI medium H	168
7.24	Elastic coefficients for TTI media	169
7.25	2-D Green's function solutions for homogeneous TTI medium	170
7.26	2-D solution at 170 kHz in a zinc crystal	171
7.27	2-D solution at 300 kHz in an apatite crystal	172
7.28	2-D solution at 200 kHz in an anisotropic crystal	172

7.29	3-D Orthorhombic medium, x - z planes	173
7.30	3-D Orthorhombic medium, x - z planes	174
7.31	3-D Orthorhombic medium, x - y planes	175
7.32	3-D Orthorhombic medium, x - y planes	176
7.33	3-D Orthorhombic medium, y - z planes	177
7.34	3-D Orthorhombic medium, y - z planes	178
7.35	Model for free surface modelling	179
7.36	Free surface modelling with buried source	179
7.37	A simple inhomogeneous model	180
7.38	Inhomogeneous media A,B, z -directed source	182
7.39	Inhomogeneous media A,B, y -directed source	183
7.40	Inhomogeneous isotropic raytracing results	184
7.41	Inhomogeneous VTI media E,F, y -directed source in E	185
7.42	Inhomogeneous VTI media, raytracing results	186
7.43	Inhomogeneous VTI media F,E, y -directed source in F	187
7.44	Inhomogeneous VTI media, raytracing results	188
7.45	2-D time-domain snapshot (homogeneous, isotropic medium A)	190
7.46	2-D time-domain snapshot (homogeneous, isotropic medium A)	190
7.47	2-D time-domain snapshot (homogeneous, isotropic medium C)	191
7.48	2-D time-domain solution (homogeneous, isotropic medium C)	191
7.49	Pattern of first motion compressions and rarefactions	192
7.50	2-D time-domain snapshot (homogeneous, VTI)	192
7.51	2-D time-domain solution for zinc crystal	193
7.52	2-D time-domain solution for apatite crystal	194
7.53	2-D time-domain solution for an anisotropic crystal	195
7.54	2-D time-domain solution for another anisotropic crystal	196
7.55	2-D time-domain solution for heterogeneous VTI medium	197
7.56	Labelling of wave modes for heterogeneous medium	198
7.57	Mode conversions at an interface	200
7.58	2-D time-domain solution (homogeneous, isotropic)	201
7.59	2-D time-domain solution (homogeneous, isotropic)	202
7.60	2-D time-domain solution (homogeneous, isotropic)	202
7.61	2-D time-domain solution (homogeneous, isotropic)	203
7.62	2-D time-domain solution (homogeneous, VTI)	203
7.63	Split parts of the time-domain solution	204
7.64	PML damping normal to interface)	205
7.65	Moderate success of viscous boundary conditions	206
7.66	Failure of viscous boundary conditions	206
7.67	Success of decomposed gradient PML at low wavenumbers	207
7.68	Success of simple PML at low wavenumbers	207
7.69	Success of decomposed gradient PML at higher wavenumbers	208
7.70	Success of simple PML at high wavenumbers	208
7.71	Evaluation of PMLs in Natural Nulls	209
7.72	Performance of the decomposed gradient PML for zinc crystal	210
7.73	Performance of the simple PML for zinc crystal	211
7.74	Performance of decomposed gradient PMLs with wider boundary.	211
7.75	Instability of the time-domain PML	212

7.76	The nonzero values in the system matrix - frequency-domain	213
7.77	The nonzero values in the system matrix - time-domain	214
7.78	Memory usage frequency-domain vs. time-domain	215
8.1	Evanescent energy past cutoff wavenumber	220
8.2	Evanescent energy in a VTI medium	221
8.3	Oscillatory behaviour in the frequency-wavenumber domain	224
8.4	Spreading of wavefield solutions as wavenumber increases	225
8.5	Critical wavenumbers in isotropic medium D	227
8.6	Critical wavenumbers in a VTI medium	228
8.7	Phase and group velocities in a VTI medium	229
8.8	Phase and group velocities in a VTI medium	232
8.9	Critical wavenumbers in a VTI medium at varying angles	234
8.10	Critical wavenumbers in a TTI medium at varying angles, x-directed	235
8.11	Critical wavenumbers in a TTI medium at varying angles, y-directed	236
8.12	Critical wavenumbers in a TTI medium at varying angles, z-directed	237
8.13	Critical wavenumbers in a VTI medium at varying angles	238
8.14	Zooming in on critical wavenumbers, y,x component, VTI analytic solution	239
8.15	A simple inhomogeneous model	240
8.16	Wavenumber spectrum, mediums AB, source in B (inhomogeneous, isotropic)	241
8.17	Wavenumber spectrum, mediums AB, source in A (inhomogeneous, isotropic)	242
8.18	Critical wavenumbers in a two-layer model, source in D	244
8.19	Critical wavenumbers in a two-layer model, source in A	247
8.20	A three-layer inhomogeneous model	248
8.21	Critical wavenumbers in 3-layer model, source in D	249
8.22	Wavenumber spectrum, mediums EF, source in E (inhomogeneous, VTI)	250
8.23	Wavenumber spectrum, mediums EF, source in F (inhomogeneous, VTI)	251
8.24	Spectra of inhomogeneous with homogeneous isotropic media	252
8.25	Spectra of inhomogeneous and homogeneous VTI media	253
8.26	Analytic and IFT'd numeric solutions using 32 wavenumber samples	255
8.27	Sampling at the critical wavenumber	256
8.28	Analytic solution and IFT'd numeric using 128,256,512 wavenumber samples	260
8.29	Analytic solution and IFT'd numeric using 128,256,512 wavenumber samples	261
8.30	Analytic solution and IFT'd numeric using 32,64,128 wavenumber samples VTI medium	262
8.31	Sampling skips the critical wavenumber	263
8.32	Agreement between analytic and numeric solutions in ky domain	263
8.33	Differences between analytic and numeric at critical wavenumbers	264
8.34	Analytic solution and IFT'd numeric skipping critical wavenumbers	265
8.35	Analytic solution and IFT'd numeric using GL wavenumber spacings	266
8.36	Time-wavenumber domain plots	267
A.1	Equi-spaced and GLL spaced models	274
A.2	Equi-spaced versus GLL-spaced quadrature	275
A.3	The Runge effect	276
C.1	Boundary integrals	280

F.1	Slices of the 3-D analytic solution (homogeneous, isotropic)	288
F.2	Isotropic frequency-domain analytic solution in plane 6m from source . . .	289
F.3	Slices of the 3-D analytic solution (homogeneous, isotropic)	289
F.4	Isotropic frequency-domain analytic solution in plane 6m from source . . .	290
F.5	Slices of the 3-D analytic solution (homogeneous, isotropic)	290
F.6	Isotropic frequency-domain analytic solution in plane containing source . .	291
F.7	Isotropic frequency-domain analytic solution for a sweep of frequencies . .	291
F.8	Slices of the 3-D analytic solution (homogeneous, VTI)	292
F.9	Slices of the 3-D analytic solution (homogeneous, VTI)	292
F.10	Slices of the 3-D analytic solution (homogeneous, VTI)	293
F.11	Phase and group velocities in a VTI medium	294
F.12	VTI frequency-domain analytic solution for a sweep of frequencies	295
H.1	Attenuated wavenumber spectra (real)	308
H.2	Attenuated wavenumber spectra (imaginary)	309
H.3	Attenuated wavenumber domain solutions (real)	310
H.4	Attenuated wavenumber domain solutions (imaginary)	311
H.5	Real IFT'd attenuated solutions	312
H.6	Imaginary IFT'd attenuated solutions	313

Abstract

Forward modelling of seismic waves is an essential tool in the determination of the underlying structure of the Earth using inversion techniques. Despite recent advances in computer power and memory resources, full 3-D elastic wave modelling continues to place a heavy burden on a typical personal computer. 2.5-D modelling reduces the computational burden while maintaining 3-D wavefield characteristics. In this thesis I present 2.5-D frequency-domain equations of motion for elastic wave modelling in anisotropic media. The reduced set of equations for vertical transversely isotropic media and tilted transversely isotropic media are presented separately. Using the spectral-element method, I develop the equations of motion into readily implemented sub-equations by identifying simple 1-D and 2-D patterns.

Some aspects of my computational implementation are unique, in particular the use of a system of dynamically growing binary trees to serve as a system matrix. Using this system, the matrix is automatically stored in compressed row format. I investigate the use of both distributed memory and shared memory supercomputers for 3-D modelling and compare the resource use of various matrix solvers.

In this thesis I adapt recently developed Perfectly Matched Layer formulations to the 2.5-D elastic case, and find them to be adequate in most situations. I investigate the possibility of instability in the absorbing layers.

Observation of 2.5-D modelling results in the frequency-wavenumber domain uncovers pole-like behaviour at critical wavenumbers within the spectrum. I demonstrate how this behaviour threatens the accuracy of the inverse Fourier transformed frequency-domain solution. However for inhomogeneous media, under certain conditions the only medium that exhibits pole-like behaviour is the medium containing the source. Further study of the phenomenon shows that in homogeneous, transversely isotropic media, the critical wavenumber values are not dependent on the receiver position, but rather can be predicted using the maximum phase velocities of the media.

The recommended strategy for wavenumber sampling is to use dense even spacing of values,

to adequately capture the behaviour close to the critical wavenumbers. A further recommendation is to introduce slight attenuation through the use of complex velocities (or elastic constants) to eliminate any pole-like behaviour at the critical values.

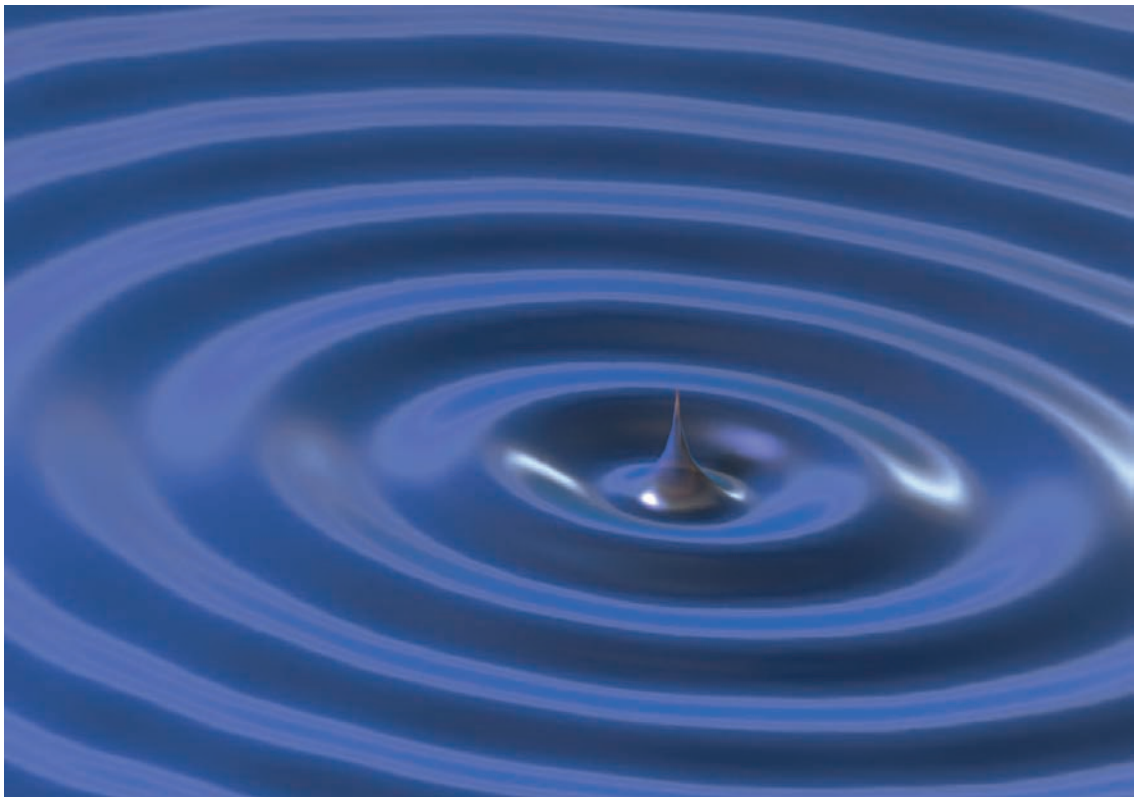
Statement

This work contains no material which has been accepted for the award of any other degree or diploma in any university or other tertiary institution to Catherine Ellen Sinclair and, to the best of my knowledge and belief, contains no material previously published or written by another person, except where due reference has been made in the text.

I give consent to this copy of my thesis, when deposited in the University Library, being made available for loan and photocopying, subject to the provisions of the Copyright Act 1968.

I also give permission for the digital version of my thesis to be made available on the web, via the University's digital research repository, the library catalogue, the Australasian Digital Thesis Program (ADTP) and also through web search engines, unless permission has been granted by the University to restrict access for a period of time

Catherine Sinclair
June 2009



To my husband Bruce.

Acknowledgements

I sincerely thank my two supervisors Professor Stewart Greenhalgh and Doctor Bing Zhou. Professor Greenhalgh provided me with a theoretical foundation for my research and shared his deep understanding and experience of many aspects of geophysics. Doctor Zhou provided great guidance and inspiration. I thank my colleagues Mark Greenhalgh, Xu Liu and Timothy Wiese for their advice and support, particularly when the going got tough. Thanks also to Sabine Latzel and Edgar Manukyan of the Institute of Geophysics ETH Zurich, Switzerland for their valuable feedback and assistance.

My research would not have been possible without the technical support and supercomputer resources of eResearch SA.

I thank the developers of the software packages SuperLU, CHOLMOD and PARDISO, for making their products freely available to university researchers. I am also grateful to the people who, via the internet, freely share their knowledge of L^AT_EX and C programming.

A special thanks to my family for their love and support.

My research was funded by an Australian Research Council Discovery grant and a University of Adelaide Faculty scholarship.